



3

6

³GAIA-Antártica, Universidad de Magallanes, Avda. Bulnes 01855, Punta Arenas,

13 ^{*}Corresponding author: pimoreno@uchile.cl



15 ABSTRACT

16

17 Few studies have examined in detail the sequence of events during the last glacial
18 termination (T1) the core sector of the Patagonian Ice Sheet (PIS), the largest ice mass
19 in the southern hemisphere outside Antarctica. Here we report results from Lago Edita
20 (47°8'S, 72°25'W, 570 m.a.s.l.), a small closed-basin lake located in a valley overridden by
21 eastward-flowing Andean glaciers during the Last Glacial Maximum (LGM). Lago Edita
22 shows glaciolacustrine sedimentation until 19,400 yr BP and a mosaic of cold-resistant,
23 hygrophilous conifers and rainforest trees, along with alpine herbs between 19,000-
24 19,400 yr BP. Increases in arboreal pollen at 13,200 and 11,000 yr BP led to the
25 establishment of forests near Lago Edita between 9000-10,000 yr BP. Our data suggest
26 that the PIS retreated at least ~90 km from its LGM limit between ~19,400-11,000 yr BP
27 and that scattered, low-density populations of cold-resistant hygrophilous conifers,
28 rainforest trees, high Andean and steppe herbs thrived east of the Andes during the LGM
29 and T1, implying high precipitation and SWW intensity at 47°S. We interpret large-
30 magnitude increases in arboreal vegetation as treeline-rise episodes driven by warming
31 pulses at 13,200 and 11,000 yr BP coupled with a decline in SWW influence at ~11,000 yr
32 BP, judging from the disappearance of cold-resistant hygrophilous trees and herbs. We
33 propose that the PIS imposed a regional cooling signal along its eastern, downwind margin
34 through T1 that lasted until the separation of the North and South Patagonian icefields
35 along the Andes. We posit that the withdrawal of glacial and associated glaciolacustrine
36 environments through T1 provided a route for the dispersal of hygrophilous trees and
37 herbs from the eastern flank of the central Patagonian Andes, contributing to the
38 afforestation of the western Andean slopes and pacific coasts of central Patagonia during
39 T1.

40



41 INTRODUCTION

42

43 The Patagonian ice sheet (PIS) was the largest ice mass in the southern hemisphere
44 outside Antarctica during the last glacial maximum (LGM). Outlet lobes from the PIS
45 flowed westward into the Pacific coast south of 43°S and eastward toward the extra-
46 Andean Patagonian plains, blanketing a broad range of environments and climatic zones
47 across and along the Andes. Land biota from formerly ice-free sectors underwent local
48 extinction or migrated toward the periphery of the advancing PIS during the last glaciation
49 until its culmination during the LGM. The PIS then underwent rapid recession and thinning
50 through the last glacial termination (termination 1= T1: between ~11,000-18,000 yr BP)
51 toward the Andes as illustrated by stratigraphic, geomorphic and radiocarbon-based
52 chronologies from northwestern Patagonia (39°-43°S) (Denton et al., 1999; Moreno et al.,
53 2015). These data, along with the Canal de la Puntilla-Huelmo pollen record (Moreno et
54 al., 2015), indicate abandonment from the LGM margins in the lowlands at 17,800 yr BP
55 and accelerated retreat that exposed Andean cirques located above 800 m.a.s.l. within
56 1000 years or less in response to abrupt warming. Similarly, glaciers from Cordillera
57 Darwin (54°-55°S), the southernmost icefield in South America, underwent rapid
58 recession from their LGM moraines located in central and northern Tierra del Fuego prior
59 to 17,500 yr BP, and led to ice-free conditions by 16,800 yr BP near the modern ice fronts
60 (Hall et al., 2013)

61 Because very few studies have been conducted in the continental sector of central-
62 west Patagonia (45°-48°S) it is yet unclear (i) the timing of the LGM and the
63 structure/chronology of glacial retreat, (ii) the timing, structure and rates of climate
64 changes during T1, as well as the (iii) composition of the vegetation that thrived adjacent
65 to the LGM margins, (iv) the tempo and mode of vegetation colonization at site-specific
66 scale, and (v) at regional scale through the increasingly ice-free Patagonian landscapes
67 during T1. The latter is important for identifying possible glacial refugia and the dispersal
68 routes of the vegetation following the LGM.



69 Paleoclimate simulations (Bromwich et al., 2005; Bromwich et al., 2004) and
70 stratigraphic studies (Kaufman et al., 2004) in the periphery of the Laurentide Ice Sheet in
71 North America, have detected that large ice sheets exerted important impacts on the
72 thermal structure and atmospheric circulation at regional, continental and zonal scale
73 from the LGM to the early Holocene. This aspect has remained largely unexplored in the
74 PIS region, and might be a factor of importance for understanding the dynamics of the
75 SWW and climatic/biogeographic heterogeneities through T1 at regional scale. Progress in
76 this field requires understanding the deglacial chronology of the PIS and a suite of
77 sensitive paleoclimate sites across and along the residual ice masses through the last
78 transition from extreme glacial to extreme interglacial conditions.

79 Recent chronologies based on cosmogenic radio nuclides of terminal moraines of
80 the Río Blanco and recessional moraines deposited by the Lago Cochrane ice lobe (LCIL)
81 (Boex et al., 2013; Hein et al., 2010) (Figure 1), and optically stimulated luminescence
82 dating of glaciolacustrine beds associated with Glacial Lake Cochrane (GLC) (47°S) (Glasser
83 et al., 2016) reported ages of 29,000 yr BP for the final LGM advance and an interval
84 between 8000-13,000 yr BP for the subsequent drainage of GLC toward the Pacific, event
85 that took place when enough glacial recession and thinning breached the continuity that
86 the North and South Patagonian Icefields achieved during the LGM (Turner et al., 2005).
87 Palynological interpretations from the Lago Shaman and Mallín Pollux sites (de Porras et
88 al., 2012; Markgraf et al., 2007), located east of the Andes between 44°S and 45°S
89 respectively (Figure 1), indicate predominance of cold and dry conditions during T1
90 negative anomalies in southern westerly wind (SWW) influence. The validity and regional
91 applicability of these stratigraphic, chronologic and palynologic interpretations, however,
92 awaits replication by detailed stratigraphic/geomorphic data from sensitive sites
93 constrained by precise chronologies.

94 In this study we report high-resolution pollen and macroscopic charcoal records
95 from sediment cores we collected in Lago Edita (47°8'S, 72°25'W, ~570 m.a.s.l.), a small
96 closed-basin lake located in Valle Chacabuco, east of the central Patagonian Andes (Figure
97 1). Stratigraphic and chronologic results from Valle Chacabuco are important for



98 elucidating the timing and rates of deglaciation in this core region of the PIS because this
 99 valley is located approximately two thirds (90 km) upstream from the LGM moraines
 100 deposited by LCIL east of Lago Cochrane relative to the modern ice fronts, and its
 101 elevation spans the highest levels of GLC during T1. The Lago Edita data allow assessment
 102 of vegetation, fire-regime and climate changes during the last global transition from
 103 extreme glacial to extreme interglacial conditions in central-west Patagonia. The aim of
 104 this paper is to contribute toward: (1) the development of a recessional chronology of the
 105 LCIL and (2) regressive phases of GLC, (3) documenting the composition and geographic
 106 shifts of the glacial and deglacial vegetation, (4) understanding the tempo and mode of
 107 vegetation and climate changes during T1 and the early Holocene, (5) constraining the
 108 regional climatic influence of the PIS during T1 in terrestrial environments, and (6)
 109 identifying possible dispersal routes of tree taxa characteristic of modern evergreen
 110 forests in central-west Patagonia during T1.

111

112 Study Area


113



114 Central Chilean Patagonia, i.e. the Aysén region (43°45'S-47°45'S), includes
 115 numerous channels, fjords, islands, and archipelagos along the Pacific side, attesting for
 116 tectonic subsidence of Cordillera de la Costa and intense glacial erosion during the
 117 Quaternary. The central sector features an intricate relief associated to the Patagonian
 118 Andes with summits surpassing 3000 m.a.s.l., deep valleys, lakes of glacial origin, and
 119 active volcanoes such as Hudson, Macá, Cay, Mentolat and Melimoyu (Stern, 2004). The
 120 Andes harbors numerous glaciers and the North Patagonian Icefield (Figure 1), which
 121 acted as the source for multiple outlet glacier lobes that coalesced with glaciers from the
 122 South Patagonian Icefield and formed the PIS during Quaternary glaciations, blocked the
 123 drainage toward the Pacific and changed the continental divide in the region (Turner et
 124 al., 2005). Farther to the east the landscape transitions into the back-arc extra-Andean
 125 plains and plateaus.



126 Patagonia is ideal for studying the paleoclimate evolution of the southern mid-
 127 latitudes including past changes in the SWW because it is the sole continental landmass
 128 that intersects the low and mid-elevation zonal atmospheric flow south of 47°S.
 129 Orographic rains associated to storms embedded in the SWW enhance local precipitation
 130 by the ascent of moisture-laden air masses along the western Andean slopes, giving way
 131 to subsidence and acceleration of moisture-deprived winds along the eastern Andean
 132 slopes (Garreaud et al., 2013). This process accounts for a steep precipitation gradient
 133 across the Andes, illustrated by the annual precipitation measured in the coastal township
 134 of Puerto Aysén (2414 mm/year) and the inland Balmaceda (555 mm/year)
 135 (<http://explorador.cr2.cl/>), localities separated by ~80 km along a west-to-east axis. The
 136 town of Cochrane, located ~15 km south of our study site features annual precipitation of
 137 680 mm/year and mean annual temperature of 7.8 °C (Figure 1).

138 Weather station and reanalysis data along western Patagonia show positive
 139 correlations between zonal wind speed and local precipitation, a relationship that extends
 140 to sectors adjacent to the eastern slopes of the Andes (Garreaud et al., 2013; Moreno et
 141 al., 2014). Therefore, changes in local precipitation in the Aysén region are good
 142 diagnostics for atmospheric circulation changes associated with the frequency/intensity of
 143 storms embedded in the SWW over a large portion of the southeast Pacific. This
 144 relationship can be applied to paleoclimate records from central Chilean Patagonia for
 145 inferring the behavior of the SWW on the basis of past changes in precipitation or
 146 hydrologic balance. 

147 The steep precipitation gradient, in conjunction with adiabatic cooling and enhanced
 148 continentality toward the east, influences the distribution and composition of the
 149 vegetation, inducing altitudinal, latitudinal and longitudinal zonation of plant communities
 150 throughout the Patagonian Andes. Physiognomic and floristic studies (Gajardo, 1994;
 151 Luebert and Pliscoff, 2006; Pisano, 1997; Schmithüsen, 1956) have recognized five units or
 152 communities which we characterize succinctly in the following sentences: 1) Magellanic
 153 Moorland: this unit occurs in maritime sectors with high precipitation (3000-4000
 154 mm/year and low seasonality) along the islands, fjords and channels, it is dominated by



155 cushion-forming plants such as *Donatia fascicularis*, *Astelia pumila* and *Tetroncium*
 156 *magallanicum*. Also present are the hygrophilous cold-resistant trees *Nothofagus*
 157 *betuloides* and the conifers *Pilgerodendron uviferum*, *Lepidothamnus fonkii* and
 158 *Podocarpus nubigena*. 2) Evergreen rainforest: present in humid, temperate (1500 -3000
 159 mm/year; <600 m.a.s.l.) sectors of Aysén, this unit is characterized by the trees
 160 *Nothofagus nitida*, *N. betuloides*, *Drimys winteri*, along with *P. uviferum* in waterlogged
 161 environments. 3) Winter deciduous forests: located in relatively cooler and/or drier
 162 sectors with higher seasonality (400-1000 mm/year; 500-1250 m.a.s.l.). The dominant tree
 163 is *Nothofagus pumilio*, which intermingles with *N. betuloides* in western sites and the
 164 Patagonian steppe eastward. In the latter *N. pumilio* forms monospecific stands and
 165 presents a species-poor understory. 4) Patagonian steppe: occurs in substantially drier
 166 (<500 mm/year) lowland areas with heightened continentality. This unit is dominated by
 167 herbs of the families Poaceae (*Festuca*, *Deschampsia*, *Stipa*, *Hordeum*, *Rytidosperma*,
 168 *Bromus*, *Elymus*), Rubiaceae (*Galium*), and shrubs of families Apiaceae (*Mulinum*),
 169 Rosaceae (*Acaena*), Fabaceae (*Adesmia*) and Rhamnaceae (*Discaria*). 5) High Andean
 170 Desert: occurs in the wind-swept montane environments above the treeline (>1000
 171 m.a.s.l.) and is represented by herbs of the families Poaceae (*Poa*, *Festuca*), Asteraceae
 172 (*Nassauvia*, *Senecio*, *Perezia*), Berberidaceae (*Berberis*), Brassicaceae (*Cardamine*),
 173 Santalaceae (*Nanodea*), Rubiaceae (*Oreopulus*) Apiaceae (*Bolax*), Ericaceae (*Gaultheria*,
 174 *Empetrum*), along with *Gunnera magellanica* and *Valeriana*, with occasional patches of
 175 *Nothofagus antarctica*.

177 MATERIALS AND METHODS

179 We collected overlapping sediment cores over the deepest sector of Lago Edita (8 m
 180 water depth) from an anchored coring rig equipped with 10-cm diameter aluminum casing
 181 tube, using a 5-cm diameter Wright piston corer and a 7.5-cm diameter sediment-water
 182 interface piston corer with a transparent plastic chamber. We characterized the
 183 stratigraphy through visual descriptions, digital X radiographs to identify stratigraphic



184 structures and loss-on-ignition to quantify the amount of organic, carbonate and
 185 siliciclastic components in the sediments (Heiri et al., 2001).

186 The chronology of the record is constrained by AMS radiocarbon dates on bulk
 187 sediment and chronostratigraphic correlation of the H1 tephra from Volcán Hudson (Stern
 188 et al., 2016). The radiocarbon dates were calibrated to calendar years before present (yr
 189 BP) using the CALIB 7.0 program. We developed a Bayesian age model using the Bacon
 190 package for R (Blaauw and Christen, 2011) to assign interpolated ages and confidence
 191 intervals for each level analyzed.

192 We processed and analyzed continuous/contiguous sediment samples (2 or
 193 pollen and fossil charcoal. The samples were processed using a standard procedure that
 194 includes 1% KOH, sieving with a 120 µm mesh, 46% HF and acetolysis (Faegri and Iversen,
 195 1989). We added exotic *Lycopodium* spores tablets to calculate concentration
 196 (particles*cc) and accumulation rates of pollen and microscopic charcoal (particles*cm⁻²*years⁻¹)
 197 from each level. We counted between 200-300 pollen grains produced by trees,
 198 shrubs and herbs (terrestrial pollen) for each palynological sample and calculated the
 199 percent abundance of each terrestrial taxon relative to this sum. The percentage of
 200 aquatic plants was calculated in reference to the total pollen sum (terrestrial + aquatic
 201 pollen) and the percentage of ferns from the total pollen and spores sum. Zonation of the
 202 pollen record was aided by a stratigraphically constrained cluster analysis on all terrestrial
 203 pollen taxa having ≥2%, after recalculating sums and percentages.

204 We identified the palynomorphs based on a modern reference collection housed at
 205 the laboratory of Quaternary Paleoecology of Universidad de Chile, along with published
 206 descriptions and keys (Heusser, 1971). In most cases the identification was done at family
 207 or genus level, in some cases to the species level (*Podocarpus nubigena*, *Drimys winteri*,
 208 *Gunnera magellanica*, *Lycopodium magellanicum*). The palynomorph *Nothofagus dombeyi*
 209 type includes the species *N. antarctica*, *N. pumilio*, *N. betuloides* and *N. dombeyi*, the
 210 morphotype *Fitzroya/Pilgerodendron* includes the cupressaceous conifers *Fitzroya*
 211 *cupressoides* and *Pilgerodendron uviferum*.



212 We tallied microscopic ($<120\ \mu\text{m}$) and macroscopic ($>106\ \mu\text{m}$) charcoal particles to
213 document regional and local fire events, respectively. Microscopic particles were counted
214 from each pollen slide, while macroscopic charcoal was counted from 2-cc sediment
215 samples obtained from 1-cm thick and continuous-contiguous sections. The samples were
216 prepared using a standard procedure which involves deflocculation in 10% KOH, careful
217 sieving through 106 and 212 μm -diameter meshes to avoid rupture of individual particles,
218 followed by visual inspection on a ZEISS KL 1500 LCD stereoscope at 10x magnification.
219 These results were analyzed by a time-series analysis to detect local fire events using the
220 CharAnalysis software (Higuera et al., 2009), interpolating samples at regular time interval
221 based in the median time resolution of the record. We deconvoluted the CHAR signal into
222 a peaks and background component using a lowess robust to outliers smoothing with a
223 100-yr window width. We calculated locally defined thresholds to identify statistically
224 significant charcoal peaks or local fires events (99th percentile of a Gaussian distribution).

225

226 RESULTS

227

228 The sediment stratigraphy (Figure 2) reveals a basal unit of blue-gray mud between
229 819-1726 cm, horizontally laminated for the most part, in some sectors massive and
230 sandier with small amounts of granule and gravel immersed in a clayey matrix (segment
231 PC0902AT9). These inorganic clays are overlain by organic silt between 678-810 cm and
232 organic-rich lake mud (gytjja) in the topmost 678 cm. We found laminated carbonates
233 between 759-794 and 389-394 cm, for the remainder of the record carbonate values are
234 negligible or null. The record includes 2 tephras between 628-630 and 643-661 cm, which
235 exhibit sharp horizontal contacts with the over and underlying mud and, consequently, we
236 interpret them as aerial fallout deposits from explosive events originated from Volcán
237 Hudson (H1 tephra) and from Volcán Mentolat (M1 tephra) based on geochemical data,
238 respectively (Stern et al., 2016).

239 The radiocarbon results show an approximately linear increase of age with depth
240 between 9000-19,000 yr BP (Figure 3) which, in conjunction with the sediment



241 stratigraphy, suggests undisturbed in-situ pelagic deposition of lake mud and tephras in
 242 the Lago Edita basin. This study focuses on the interval between 9000-19,000 yr BP (Figure
 243 2, Table 1), and consists of 155 contiguous palynological and macroscopic charcoal levels
 244 with a median time step of 65 years between analyzed samples.

245

246 Pollen stratigraphy

247

248 We divided the record in 6 zones to facilitate its description and discussion, based
 249 on conspicuous changes in the pollen stratigraphy and a stratigraphically constrained
 250 cluster analysis (Figure 4). The following section describes each pollen zone indicating the
 251 stratigraphic and chronologic range, and the mean abundance of major taxa in
 252 parenthesis.

253 Zone Edita-1 (780-795 cm; 18,100-19,000 yr BP) is co-dominated by Poaceae (33%)
 254 and *Empetrum* (32%). This zone starts with a gradual increase in *Empetrum*, attaining its
 255 maximum abundance (~53%) at the end of this zone. Asteraceae subfamily Asteroideae
 256 (7%), *Acaena* (4%), Caryophyllaceae (3%) and Cyperaceae (9%) decrease, while Poaceae
 257 shows fluctuations in its abundance between 2-16 % over the entire interval. Other herbs
 258 and shrubs such as Ericaceae (3%), *Phacelia* (~2%), *Valeriana* (1%), *Gunnera magellanica*
 259 (~2%), Apiaceae (<1%), and Asteraceae subfamily Cichorioideae (<1%) remain relatively
 260 steady. The arboreal taxa *N. dombeyi* type (10%), *Fitzroya/Pilgerodendron* (2%), *P.*
 261 *nubigena* (<1%) and *D. winteri* (<1%) are present in low abundance, as well as the ferns *L.*
 262 *magellanicum* (~1%) and *Blechnum* type (5%) and the green-microalgae *Pediastrum* (2%).

263 Zone Edita-2 (758-780 cm; 16,800-18,100 yr BP) begins with a decline in *Empetrum*
 264 (30%) and an increase in Poaceae (34%) followed by its decrease until the end of this zone.
 265 *N. dombeyi* type (15%), Caryophyllaceae (5%) and Asteraceae subfamily Asteroideae (5%)
 266 show a rising trend during this zone, while other arboreal taxa (*Fitzroya/Pilgerodendron*
 267 (3%), *P. nubigena* (<1%) and *D. winteri* (<1%) and most of the herbs maintain similar
 268 abundance the previous zone. *L. magellanicum* (2%) and *Pediastrum* (4%) rise slightly,
 269 along with high variability in Cyperaceae (7%).



270 Zone Edita-3 (701-758 cm; 13,200-16,800 yr BP) is characterized by a sharp rise in
 271 Poaceae (45%) and declining trend in *Empetrum* (15%). The conifer *P. nubigena* (2%) starts
 272 a sustained increase, while *N. dombeyi* type (13%) and *Fitzroya/Pilgerodendron* (3%)
 273 remain relatively invariant. *D. winteri* (<1%) and *Misodendrum* (<1%), a mistletoe that
 274 grows on *Nothofagus* species, appear in low abundance in an intermittent manner.
 275 *Pediastrum* (30%) shows a rapid increase until 15,600 yr BP, followed by considerable
 276 variations in its abundance until the end of this zone (between 19% and 55%). *L.*
 277 *magellanicum* (3%) shows a steady increase, while *Blechnum* type (6%) remains invariant
 278 and Cyperaceae (7%) exhibits large fluctuations superimposed upon a declining trend.

279 Zone Edita-4 (681-701 cm; 11,600-13,200 yr BP) starts with step increases in *N.*
 280 *dombeyi* type (29%) and *Misodendrum* (1%). *P. nubigena* (5%) starts this zone with
 281 variability and stabilizes toward the end of this zone, concurrent with
 282 *Fitzroya/Pilgerodendron* (3%) and traces of *D. winteri* (<1%). Poaceae (38%) shows a
 283 steady decrease, while *Empetrum* (6%) continues with a declining trend that started
 284 during the previous zone. Asteraceae subfamily Asteroideae (5%) and Caryophyllaceae
 285 (2%) decrease, *L. magellanicum* (3%), Cyperaceae (4%) and *Pediastrum* (24%) decline
 286 gradually with considerable fluctuations, while *Blechnum*- type (11%) shows modest
 287 increases.

288 Zone Edita-5 (674-681 cm; 11,100-11,600 yr BP) shows a marked decline in *N.*
 289 *dombeyi* type (27%), *Misodendrum* (<1%) and Poaceae (33%) in concert with a
 290 conspicuous increase in the conifers *Fitzroya/Pilgerodendron* (12%) and *P. nubigena* (9%)
 291 that reach their peak abundance in the record. The abundance of herbs and shrubs
 292 decreases or remains steady, with the exception of an ephemeral increase in *Phacelia*
 293 (3%). *Blechnum* type (39%) shows a remarkable increase to its peak abundance in the
 294 entire record, while *L. magellanicum* (3%), Cyperaceae (8%) and *Pediastrum* (17%) rise
 295 slightly.

296 Zone Edita-6 (640-674 cm; 8940-11,100 yr BP) is characterized by an abrupt increase
 297 in *N. dombeyi* type (62%) and *Misodendrum* (2%), along with conspicuous decline in
 298 *Fitzroya/Pilgerodendron* (2%) and *P. nubigena* (2%) at the beginning of this zone. Poaceae



(26%) shows a downward trend over this period, while others herbs and shrubs (*Empetrum*, Ericaceae, Caryophyllaceae, Asteraceae subfamily Asteroideae, *Acaena*, *Phacelia*, *Valeriana*, *Gunnera magellanica*, Apiaceae and Asteraceae subf. Cichorioideae) show their lowest abundance in the record. *Blechnum* type (7%) drops sharply, followed by a gradual decline in concert with *L. magellanicum* (1%). Cyperaceae (7%) and *Pediastrum* (6%) show initial declines followed by increases toward the end of this zone.

Charcoal stratigraphy

The record from Lago Edita shows absence of macroscopic charcoal particles between 14,300-19,000 yr BP followed by an increase in charcoal accumulation rate (CHAR) that led to a variable plateau between 12,000-13,200 yr BP, a 1000-year long decline, and a sustained increase led to peak abundance at 9700 yr BP. Charcoal values then declined rapidly to intermediate levels by 9000 yr BP. We note a close correspondence between the *Nothofagus* abundance (%) and the CHAR suggesting that charcoal production was highly dependent upon quantity and spatial continuity of coarse woody fuels in the landscape (Figure 5).

Time-series analysis of the macroscopic charcoal record revealed 11 statistically significant peaks we interpret as local fires events within the Lago Edita watershed (Figure 5). The temporal structure of these events indicates a sequence of millennial-scale peaks in fire frequency with maxima at 9600, 10,900, 12,000, 13,100, and 14,100 yr BP. We observe a steady increase in the fire frequency maxima from 14,100 to 10,900 yr BP (Figure 5).

DISCUSSION

Paleovegetation

The pollen record from Lago Edita (Figures 4, 6) documents dominance of herbs and shrubs (chiefly Poaceae, *Empetrum*, Asteraceae, accompanied by Caryophyllaceae,



328 *Acaena*, Ericaceae, *Phacelia*, *Valeriana*, and Apiaceae in lower abundance) found above
 329 the modern treeline and the Patagonian steppe between 11,000-19,000 yr BP, followed by
 330 increasing *Nothofagus* we interpret as the establishment of scrubland (11,000-13,200 yr
 331 BP), woodland (10,500-11,000 yr BP) and forest (9000-10,500 yr BP). Within the interval
 332 dominated by non-arboreal taxa we distinguish an initial phase with abundant *Empetrum*
 333 between 16,800-19,000 yr BP, followed by diversification of the herbaceous assemblage
 334 and preeminence of Poaceae during the interval 11,000-16,800 yr BP (Figures 4, 6). This
 335 change is contemporaneous with a sustained rise of *P. nubigena* and the mistletoe
 336 *Misodendrum* coeval with conspicuous increases in *Lycopodium magellanicum* and the
 337 green microalga *Pediastrum*. We emphasize the continuous presence of the arboreal
 338 *Nothofagus* and *Fitzroya/Pilgerodendron* in low but constant abundance (~15% and ~3%,
 339 respectively) between 13,000-19,000 yr BP, along with traces (<3%) of hygrophilous trees
 340 (*Podocarpus nubigena*, *Drimys winteri*) and herbs (*Gunnera magellanica*, *Lycopodium*
 341 *magellanicum*) accounting, in sum, for a persistent ~25% of the pre-13,200 yr BP pollen
 342 record (Figures 4, 6).

343 The mixed palynological assemblage between ~11,000-19,400 yr BP has no modern
 344 analogues in the regional vegetation (Luebert and Plischoff, 2006; Mancini, 2002). Possible
 345 explanations for its development involve: (a) downslope migration of High Andean
 346 vegetation driven by snowline and treeline lowering associated with intense glaciation in
 347 the region, coupled with (b) the occurrence of scattered, low-density populations of
 348 hygrophilous trees and herbs along the eastern margin of the PIS during the LGM and T1.
 349 We rule out the alternative explanation that pollen grains and spores of hygrophilous
 350 trees and herbs in Lago Edita represent an advected signal through the Andes from ice-
 351 free humid Pacific sectors harboring these species because: (i) no empirical basis is
 352 currently available for ice-free conditions and occurrence of cold-resistant hygrophilous
 353 taxa along the western Andean slopes or the Pacific coast of central Patagonia during the
 354 LGM; in fact, the oldest minimum limiting dates for ice-free conditions in records from
 355 Taitao Peninsula and the Chonos archipelago yielded ages of $14,335 \pm 140$ and
 356 $13,560 \pm 125$ ^{14}C yr BP (median age probability [MAP]: 17,458 and 16,345 yr BP),



357 respectively (Haberle and Bennett, 2004; Lumley and Switsur, 1993); (ii) the appearance of
358 *Fitzroya/Pilgerodendron* and *Podocarpus nubigena* at ~15,000 and ~14,000 yr BP,
359 respectively, occurred 4000-5000 years later in coastal Pacific sites relative to the Lago
360 Edita record (Figure 7); (iii) background levels of *Nothofagus* between 15-20% in Lago
361 Edita predate the appearance and expansion of this taxon in coastal Pacific sites and, once
362 realized, its abundance in Lago Edita did not follow the trend and magnitude observed in
363 western sites, as expected if the palynological signal in Lago Edita was attributed to long-
364 distance transport from that source (Figure 7).

365 Previous palynological studies from bogs located east of the central Patagonian
366 Andes (de Porras et al., 2012; Markgraf et al., 2007) interpreted dry conditions prior to
367 ~12,000 yr BP, based on the premise that low abundance of arboreal taxa and
368 preeminence of herbs and shrubs were indicative of Patagonian Steppe communities. The
369 glacial-to-interglacial vegetation change in those studies was interpreted as a westward
370 shift of the forest-steppe boundary brought by lower-than-present SWW influence at 44°-
371 46°S, followed by a rise in temperature and precipitation at the end of the last glaciation.
372 In contrast, the Lago Augusta site (located in Valle Chacabuco ~7 km northeast of Lago
373 Edita) (Figure 1) shows a pollen assemblage prior to 15,600 yr BP dominated by high
374 Andean herbs and shrubs, along with taxa characteristic of hyperhumid environments
375 along the Pacific coasts of central Patagonia (*Nothofagus*, *Fitzroya/Pilgerodendron*,
376 *Podocarpus nubigena*, *Saxegothaea conspicua*, *Drimys winteri*, *Dysopsis glechomoides* and
377 the ferns *Blechnum*, Hymenophyllaceae, *Cystopteris*) (Villa-Martinez et al., 2012). It
378 appears then that floristic elements of modern Patagonian forests were present in low
379 abundance and in a discontinuous manner along the eastern flank of the PIS between 44°-
380 47°S. The data shown in this paper, along with the results from Lago Augusta, suggest that
381 Valle Chacabuco harbored cryptic refugia (Bennett and Provan, 2008) of rainforest trees
382 and herbs during the interval 11,000-19,000 yr BP, therefore the interpretation of lower-
383 than-present precipitation of SWW origin in previous studies (de Porras et al., 2012;
384 Markgraf et al., 2007), is not applicable to the Valle Chacabuco area over this time
385 interval. Plant colonization of Valle Chacabuco must have started from the LGM limits



386 located east of Lago Cochrane and followed the shrinking ice masses to the west, once the
 387 newly deglaciated sectors were devoid of glaciolacustrine influence through T1.

388 Declines and virtual disappearance of the cold-resistant hygrophilous trees
 389 *Fitzroya/Pilgerodendron*, *Podocarpus nubigena* and the herbs *Gunnera magellanica* and
 390 *Lycopodium magellanicum* took place at ~11,000 yr BP in the Lago Edita record (Figures 4,
 391 6), in response to a sudden decline in precipitation. These changes were
 392 contemporaneous with a sustained rise in *Nothofagus*, decreases in all other shrubs and
 393 herbs, and a major increase in macroscopic charcoal (Figure 5), signaling an increment in
 394 arboreal cover, higher spatial continuity of coarse fuels and forest fires. We interpret this
 395 arboreal increase and fire-regime shift as driven by warming which might have triggered a
 396 treeline rise and favored the spread/densification of woody species and coarse fuels
 397 (Figures 4, 5, 6). *Nothofagus* forests (~70% abundance) established near Lago Edita
 398 between 9000-10,000 yr BP.

399

400 Deglaciation of Valle Chacabuco and the Lago Cochrane basin

401

402 Stratigraphic and chronologic results from Lago Edita are key for deciphering the
 403 evolution of Valle Chacabuco and for constraining the timing and rates of deglaciation in
 404 this core region of the PIS. Previous studies (Hein et al., 2010) indicate that Valle
 405 Chacabuco was overridden by the Lago Cochrane ice lobe (LCIL) during the LGM and
 406 deposited the Río Blanco moraines ~90 km downstream from Lago Edita, distal to the
 407 eastern end of Lago Cochrane in Argentina (Argentinian name: Lago Pueyrredón).
 408 Cosmogenic radionuclide dating on the Río Blanco moraine belts yielded ages of
 409 $19,100 \pm 700$, $22,800 \pm 1000$ and $26,000 \pm 900$ yr BP (Hein et al., 2010). Kaplan et al. (2011)
 410 recalculated these ages using a local production rate constrained by radiocarbon dates
 411 from southern Patagonia and produced ages of ~21,100, ~25,100, and ~28,700 yr BP
 412 respectively. This was followed by glacial recession starting at $17,400 \pm 700$ (recalculated
 413 age: $19,600 \pm 800$) yr BP, formation of Glacial Lake Cochrane (GLC), stabilization and
 414 deposition of the Lago Columna and Lago Posada moraines at $15,900 \pm 800$ (recalculated



age: $17,600 \pm 900$ yr BP, ~ 55 km upstream from the Río Blanco moraines (Hein et al., 2010; Kaplan et al., 2011) (Figure 1). Further glacial recession led to the westward expansion and lowering of GLC until the LCIL stabilized and deposited moraines in Lago Esmeralda between $12,800$ – $13,600$ yr BP ~ 60 km upstream from the Lago Columna and Lago Posada moraines (Turner et al., 2005). Recession from this position led to sudden drainage of GLC toward the Pacific Ocean via Río Baker, once the continuity between the North and South Patagonian icefields was breached by glacial recession and thinning. According to these data Valle Chacabuco may have been ice-free and devoid of glaciolacustrine influence after $\sim 17,600$ yr BP. More recently Boex et al. (2013) reported a cosmogenic radio nuclide-based reconstruction of vertical profile changes of the LCIL through the LGM and T1 that reveals deposition of (i) the Sierra Colorado lower limit by $28,980 \pm 1206$ yr BP which can be traced to the Río Blanco moraines, (ii) the highest summits of Cerro Oportus and Lago Columna moraines by $18,966 \pm 1917$ yr BP, and (iii) the María Elena moraine by $17,088 \pm 1542$ yr BP. According to these data Valle Chacabuco may have been ice-free after $\sim 17,000$ yr BP.


Lago Edita is a closed-basin lake located ~ 11 km east of the Cerro Tamango summit along the ridge that defines the southern edge of the Valle Chacabuco watershed (Figure 1). Lacustrine sedimentation in Lago Edita started when ice-free conditions developed in Valle Chacabuco, as the LCIL snout retreated eastward to a yet unknown position. The Lago Edita cores show 9 meters of blue-gray clays with millimeter-scale laminations, interrupted by sporadic intervals of massive pebbly mud appreciable in x radiographs and the LOI_{550} record as increases in the inorganic density data (Figure 2). We also found exposed glaciolacustrine beds and discontinuous fragments of lake terraces in the vicinity of Lago Edita, attesting for a large lake that flooded Valle Chacabuco in its entirety. Differential GPS measurements of 570 m.a.s.l. for the Lago Edita surface and 591 m.a.s.l. for a well-preserved terrace fragment located ~ 150 m directly south of Lago Edita, provide minimum-elevation constraints for GLC during this stage. The Lago Augusta site (Villa-Martínez et al., 2012), located ~ 7 km northeast of Lago Edita on the Valle Chacabuco floor




443 at 444 m.a.s.l. (Figure 1), shows 8 meters of basal glaciolacustrine mud (Figure 2) lending
444 support to our interpretation.


445 Glaciolacustrine sedimentation persisted in Lago Edita and Lago Augusta until the
446 surface elevation of GLC dropped below 570 and 444 m.a.s.l., respectively, and the closed-
447 basin lakes developed. The chronology for this event is constrained by statistically
448 identical AMS dates of $16,250 \pm 90$ and $16,020 \pm 50$ ^{14}C yr BP (UCIAMS-133418 and CAMS-
449 144454, respectively) (Table 1) from the same level in the basal portion of the organic
450 sediments in the Lago Edita record; this estimate approaches the timing for the cessation
451 of glaciolacustrine influence in Lago Augusta, radiocarbon-dated at $16,445 \pm 45$ ^{14}C yr BP
452 (CAMS-144600) (Table 1). Because we observe approximately the same age for the
453 transition from glaciolacustrine to organic-rich mud in both stratigraphies, we interpret
454 the weighted mean age of those three dates ($16,254 \pm 63$ ^{14}C yr BP, MAP: 19,426 yr BP, two
455 different laboratories) as a minimum-limiting age for ice-free conditions and nearly
456 synchronous glaciolacustrine regression from elevations 591 and 444 m.a.s.l. in Valle
457 Chacabuco. We acknowledge that Villa-Martínez et al. (2012) excluded the age of date
458 CAMS-144600 from the age model of the Lago Augusta palynological record because it
459 was anomalously old in the context of other radiocarbon dates higher up in core.

460 Comparison of the radiocarbon-dated stratigraphy from Lago Edita record with the
461 exposure-age-dated glacial geomorphology from Lago Cochrane/Pueyrredón, Valle
462 Chacabuco and surrounding mountains reveals the following:


- 463
- 464 • The geochronology for the innermost (third) belt of Río Blanco moraines ($\sim 21,100$
465 yr BP) (Hein et al., 2010; Kaplan et al., 2011), glacial deposits on the highest
466 summits of Cerro Oportus and the Lago Columna moraines ($18,966 \pm 1917$ yr BP)
467 (Boex et al., 2013) are compatible (within error) with the onset of organic
468 sedimentation in Lago Edita and Lago Augusta at 19,426 yr BP in Valle Chacabuco.
469 If correct, this implies  km recession of the LCIL from its LGM limit within ~ 1500
years.
 - 470 • Hein et al. (2010)'s chronology for the "final LGM limit", Lago Columna and Lago
471 Posada moraines are anomalously young, as well as Boex et al. (2013)'s chronology



472 for the María Elena moraine. This is because cosmogenic radio nuclide ages for
473 these landforms postdate the onset of organic sedimentation in  Edita and
474 Lago Augusta, despite being morphostratigraphically distal (older) than Valle
475 Chacabuco.

- 476 • As shown in Figure 1, Lago Edita is located along a saddle that establishes the
477 southern limit of the Río Chacabuco catchment and the northern limit of the Lago
478 Cochrane basin. According to Hein et al. (2010) the drainage divide on the eastern
479 end of Lago Cochrane/Pueyrredón basin is located at 475 m.a.s.l., therefore the
480 presence of this perched glacial lake with a surface elevation of 591 m.a.s.l.
481 requires ice dams located in the Valle Chacabuco and the Lago Cochrane basin.
482 This suggests that both valleys remained partially ice covered and that enough
483 glacier thinning and recession early during T1 enabled the development of a
484 topographically constrained glacial lake that covered Valle Chacabuco up to the
485 aforementioned saddle.
- 486 • The high stand of GLC at 591 m.a.s.l. lasted for less than 1500 years during the
487 LGM and was followed by a nearly instantaneous lake-level lowering of at least
488 ~150 m at ~19,400 yr BP in Valle Chacabuco. The abrupt large-magnitude drainage
489 event of this “predecessor lake” was recently recognized by Bourgois et al. (2016),
490 but its chronology, hydrographic and climatic implications have not been
491 addressed in the literature. 

493 Biogeographic and paleoclimatic implications

494 The persistence of scattered, low-density populations of rainforest trees and herbs
495 east of the Andes during the LGM and T1 (Figures 4, 6) implies that precipitation delivered
496 by the SWW must have been substantially higher than at present (680 mm/year measured
497 in the Cochrane meteorological station  because local precipitation in western Patagonian
498 is positively and significantly correlated with low-level zonal winds (Garreaud et al., 2013;
499 Moreno et al., 2010; Moreno et al., 2014), we propose that the SWW influence at 47°S



500 was stronger than present between 11,000-19,000 yr BP, in particular between 11,000-
 501 16,800 yr BP. Subsequent increases in arboreal vegetation, chiefly *Nothofagus*, at 11,000
 502 and 13,200 yr BP led to the establishment of forests near Lago Edita between 9000-10,000
 503 yr BP (Figures 4, 6). We interpret these increases as treeline-rise episodes driven by
 504 warming pulses coupled with a decline in SWW strength at 47°S, as suggested by the
 505 disappearance of cold-resistant hygrophilous trees and herbs at ~11,000 yr BP. We
 506 speculate that the warm pulse and decline in SWW influence at ~11,000 yr BP might
 507 account for the abandonment of early Holocene glacier margins in multiple valleys in
 508 central Patagonia (Glasser et al., 2012)

509 Four salient aspects of the Lago Edita record are relevant for deciphering the pattern
 510 and rates of climate change and dispersal routes of the vegetation in Central Patagonia
 511 (47°S) during the last glacial termination (T1):

512 1- Absence of stratigraphically discernable indications of deglacial warming
 513 between 13,200-19,400 yr BP, in contrast to northwestern Patagonian records
 514 (the Canal de la Puntilla and Huelmo sites) (Moreno et al., 2015) which show that
 515 75-80% of the glacial-interglacial temperature recovery was accomplished
 516 between 16,800-17,800 yr BP (Figure 8). The record from Lago Stibnite, located
 517 in central-west Patagonia upwind from the PIS and Lago Edita, shows a rapid
 518 increase in arboreal pollen from ~2% to >80% in less than 1000 years starting at
 519 16,200 yr BP (Figure 8). We posit that cold glacial conditions lingered along the
 520 periphery of the shrinking PIS during T1, affecting adjacent downwind sectors
 521 such as Valle Chacabuco. According to Turner et al. (2005) the LCIL stabilized and
 522 deposited moraines in Lago Esmeralda, located ~10 km upstream and ~240 m
 523 lower in elevation than Lago Edita, between 12,800-13,600 yr BP. We propose
 524 that the climatic barrier for arboreal expansion vanished in downwind sectors
 525 such as Valle Chacabuco once glacial recession from the Lago Esmeralda margin
 526 breached the continuity of the North and South Patagonian icefields along the
 527 Andes. Thus, we propose that regional cooling induced by the PIS along its



528 eastern margin through T1 accounts for the delayed warming in Valle Chacabuco
 529 relative to records located in western and northwestern sectors (Figure 8).

530 2- Cold and wet conditions prevailed between 16,800-19,400 yr BP, followed by an
 531 increase in precipitation at 16,800 yr BP. The latter event is contemporaneous
 532 with the onset of a lake-level rise in Lago Lepué (43°S, central-east Isla Grande
 533 de Chiloé) (Figure 8), which Pesce & Moreno (2014) interpreted as a northward
 534 shift of the SWW as they recovered from a prominent southward shift from
 535 latitudes ~41°-43°S (Figure 8) following the onset of T1 (Moreno et al., 2015).

536 3- Significant ice recession (~90 km) from the eastern LGM margin of the Lago
 537 Cochrane Ice lobe (LCIL) was accomplished between ~19,400-21,000 yr BP, at
 538 times when northwestern Patagonian piedmont glacier lobes experienced
 539 moderate recession during the Varas interstade (Denton et al., 1999; Moreno et
 540 al., 2015) (Figure 8). In contrast to the LCIL, northwestern Patagonian piedmont
 541 glacier lobes readvanced to their youngest glacial maximum position during a
 542 cold episode between 17,800-19,300 yr BP that featured stronger SWW
 543 influence at 41°-43°S (Moreno et al., 2015) (Figure 8). One explanation for this
 544 latitudinal difference might be that northward-shifted SWW between 17,800-
 545 19,300 yr BP fueled glacier growth in northwestern Patagonia while reducing the
 546 delivery of moisture to central Patagonia, causing the LCIL to continue the
 547 recession it had started during the Varas interstade.

548 4- A mosaic of cold-resistant and hygrophilous trees and herbs, currently found
 549 along the humid western slopes of the Andes of central Chilean Patagonia, and
 550 cold-resistant shrubs and herbs common to high-Andean and Patagonian steppe
 551 communities developed along the eastern margin of the PIS during the LGM and
 552 T1 (Figures 4, 6). We posit that glacial withdrawal and drainage of GLC through
 553 T1 provided a route for the westward dispersal of hygrophilous trees and herbs,
 554 contributing to the forestation of the newly deglaciated sectors of central-west
 555 Patagonia.



556 We conclude that warm pulses at 13,200 and 11,000 yr BP and a decline in SWW
557 influence at 47°S starting at 11,000 yr BP brought T1 to an end in central-west Patagonia.
558 The earliest of these events overlaps in timing with the culmination of Patagonian (Garcia
559 et al., 2012; Moreno et al., 2009; Strelin et al., 2011; Strelin and Malagnino, 2000) and
560 New Zealand glacier advances during the Antarctic Cold Reversal. Our data suggest that
561 the subsequent warm pulse, which was accompanied by a decline in SWW strength at
562 11,000 yr BP (Moreno et al., 2010; Moreno et al., 2012), was the decisive event that led to
563 the end of T1 in the study area.

564

565 ACKNOWLEDGEMENTS

566 This study was funded by Fondecyt #1080485, 1121141, ICM grants P05-002 and
567 NC120066, and a CONICYT M.Sc. Scholarship to W.I.H. We thank E.A. Sagredo, O.H. Pesce,
568 E. Simi, and I. Jara for assistance during field work, K.D. Bennett and S. Haberle for sharing
569 published palynological data. We thank C. Saucedo from Agencia de Conservación
570 Patagónica for permission to work and collect samples in Hacienda Valle Chacabuco
571 (Parque Patagonia).

572



573



574 FIGURE AND TABLE CAPTIONS

575 Table 1. Radiocarbon dates from the Lago Edita core. The radiocarbon dates were
 576 calibrated to calendar years before present using the CALIB 7.0 program.


577

578 Figure 1  Sketch map of the study area showing the location of central-west Patagonia, the
 579 position of Valle Chacabuco relative to the Río Blanco ice limit east Lago of Cochrane, and
 580 the North Patagonian icefield and Peninsula Taitao to the west. The lower portion of the
 581 figure shows a detail on the Cerro Tamango area and the portion of Valle Chacabuco
 582 where Lago Edita and Lago Augusta are located. Also shown are palynological sites
 583 discussed in the main text 


584

585 Figure 2. Stratigraphic column, radiocarbon dates and loss-on-ignition data from the Lago
 586 Edita record. The labels on the right indicate the identity and stratigraphic span (dashed
 587 horizontal lines) of each core segment.



588

589 Figure 3. Age model of the Lago Edita record, the blue zones represent the probability
 590 distribution of the calibrated radiocarbon dates, the grey zone represents the calculated
 591 confidence interval of the Bayesian age model 

592

593 Figure 4. Percentage pollen diagrams from the Lago Edita core. The labels on the right
 594 indicate the identity and stratigraphic span (dashed horizontal lines) of each pollen
 595 assemblage zone. The black dots indicate presence of *Drimys winteri* pollen grains,
 596 normally < 1% 

597

598 Figure 5. Macroscopic charcoal record from the Lago Edita core and results of
 599 CharA  analysis: blue line: background component, red line: locally defined threshold ,
 600 triangles: statistically significant charcoal peaks, magnitude: residual abundance that
 601 supersedes the threshold.

602



603 Figure 6. Selected palynomorph abundance of the Lago Edita record shown in the time
 604 scale domain. The red lines correspond to weighted running means of seven adjacent
 605 samples with a triangular filter. The taxa shown in the left panel are characteristic of
 606 humid environments currently found in sectors adjacent to the Pacific coast and/or the
 607 Andean treeline in the study area. The taxon *Nothofagus dombeyi* type, which includes
 608 multiple species with contrasting climatic tolerances, is also found in (relatively) humid
 609 sectors east of the Andes. The herbs and shrubs shown in the right panel are either
 610 cosmopolitan or present in the Patagonian Steppe and sectors located at or above the
 611 Andean treeline in central-west Patagonia.

612
 613 Figure 7. Comparison of selected tree pollen recorded in Lago Fácil, Lago Oprasa, Lago
 614 Stibnite (Lumley and Switsur, 1993) and Lago Edita. The red line corresponds to a
 615 weighted running mean in each record of seven adjacent samples with a triangular filter.
 616 The lower panels show the curves from all sites expressed in a common percent scale
 617 (Lago Fácil: purple line, Lago Oprasa: blue line, Lago Stibnite: black line, and Lago Edita:
 618 red line).

619
 620 Figure 8. Comparison of the percent sum of arboreal pollen (AP) in records from Lago
 621 Edita, Lago Stibnite (Lumley and Switsur, 1993) and the spliced Canal de la Puntilla-
 622 Huelmo time series (Moreno et al., 2015), as proxies for local rise in treeline driven by
 623 deglacial warming. These data are compared against the δ Deuterium record from the
 624 Antarctic Epica Dome Concordia (EDC) ice core (Stenni et al., 2010), and hydrologic
 625 estimates from northwestern Patagonia. The latter consist of the percent abundance of
 626 Magellanic Moorland species found in the spliced Canal de la Puntilla-Huelmo record
 627 (Moreno et al., 2015), indicative of a hyperhumid regime, and the percent abundance of
 628 the littoral macrophyte *Isoetes savatieri* from Lago Lepu   (Pesce and Moreno, 2014),
 629 indicative of low lake level (LL) during the earliest stages of T1 and the early Holocene
 630 (9000-11,000 yr BP). The vertical dashed lines constrain the timing of the early Holocene
 631 SWW minimum at 41  -43  S (9000-11,000 yr BP) (Fletcher and Moreno, 2011), a low-



632 precipitation phase during the early termination at 41°-43°S (16,800-17,800 yr BP)
633 associated with a southward shift of the SWW (Pesce and Moreno, 2014), the final LGM
634 advance of piedmont glacier lobes (17,800-19,300 yr BP) and the final portion of the Varas
635 interestade (19,300-21,000 yr BP) in the Chilean Lake District (Denton et al., 1999; Moreno
636 et al., 2015). The dashed green horizontal lines indicate the mean AP of each pollen record
637 prior to their increases during T1 (Lago Edita: 17%, Lago Stibnite:2%, spliced Canal de la
638 Puntilla-Huelmo: 31%). The ascending oblique arrow represents a northward shift of the
639 SWW, the descending arrow a southward shift of the SWW at the beginning of T1.
640
641



642 REFERENCES CITED

- 643 Bennett, K.D., Provan, J., 2008. What do we mean by 'refugia'? Quaternary Science Reviews 27,
644 2449-2455.
- 645 Blaauw, M., Christen, J.A., 2011. Flexible Paleoclimate Age-Depth Models Using an Autoregressive
646 Gamma Process. Bayesian Analysis 6, 457-474.
- 647 Boex, J., Fogwill, C., Harrison, S., Glasser, N.F., Hein, A., Schnabel, C., Xu, S., 2013. Rapid thinning of
648 the late Pleistocene Patagonian Ice Sheet followed migration of the Southern Westerlies.
649 Scientific reports 3.
- 650 Bourgois, J., Cisternas, M.E., Braucher, R., Bourlès, D., Frutos, J., 2016. Geomorphic Records along
651 the General Carrera (Chile)–Buenos Aires (Argentina) Glacial Lake (46°–48°S), Climate
652 Inferences, and Glacial Rebound for the Past 7–9 ka. The Journal of Geology 124, 27-53.
- 653 Bromwich, D.H., Toracinta, E.R., Oglesby, R.J., Fastook, J.L., Hughes, T.J., 2005. LGM Summer
654 Climate on the Southern Margin of the Laurentide Ice Sheet: Wet or Dry? Journal of Climate
655 18, 3317-3338.
- 656 Bromwich, D.H., Toracinta, E.R., Wei, H., Oglesby, R.J., Fastook, J.L., Hughes, T.J., 2004. Polar MM5
657 Simulations of the Winter Climate of the Laurentide Ice Sheet at the LGM. Journal of Climate
658 17, 3415-3433.
- 659 de Porras, M.E., Maldonado, A., Abarzúa, A.M., Cárdenas, M.L., Francois, J.P., Martel-Cea, A.,
660 Stern, C.R., Méndez, C., Reyes, O., 2012. Postglacial vegetation, fire and climate dynamics at
661 Central Chilean Patagonia (Lake Shaman, 44°S). Quaternary Science Reviews 50, 71-85.
- 662 Denton, G.H., Lowell, T.V., Heusser, C.J., Schluchter, C., Andersen, B.G., Heusser, L.E., Moreno, P.I.,
663 Marchant, D.R., 1999. Geomorphology, stratigraphy, and radiocarbon chronology of
664 Llanquihue drift in the area of the southern Lake District, Seno Reloncavi, and Isla Grande de
665 Chiloe, Chile. Geografiska Annaler Series a-Physical Geography 81A, 167-229.
- 666 Faegri, K., Iversen, J., 1989. Textbook of pollen analysis. John Wiley & Sons.
- 667 Fletcher, M.S., Moreno, P.I., 2011. Zonally symmetric changes in the strength and position of the
668 Southern Westerlies drove atmospheric CO₂ variations over the past 14 k.y. Geology 39,
669 419-422.
- 670 Gajardo, R., 1994. La Vegetación Natural de Chile. Clasificación y Distribución Geográfica. Editorial
671 Universitaria, Santiago, Chile.
- 672 Garcia, J.L., Kaplan, M.R., Hall, B.L., Schaefer, J.M., Vega, R.M., Schwartz, R., Finkel, R., 2012.
673 Glacier expansion in southern Patagonia throughout the Antarctic cold reversal. Geology 40,
674 859-862.
- 675 Garreaud, R., Lopez, P., Minvielle, M., Rojas, M., 2013. Large-Scale Control on the Patagonian
676 Climate. Journal of Climate 26, 215-230.
- 677 Glasser, N.F., Harrison, S., Schnabel, C., Fabel, D., Jansson, K.N., 2012. Younger Dryas and early
678 Holocene age glacier advances in Patagonia. Quaternary Science Reviews 58, 7-17.
- 679 Glasser, N.F., Jansson, K.N., Duller, G.A.T., Singarayer, J., Holloway, M., Harrison, S., 2016. Glacial
680 lake drainage in Patagonia (13-8 kyr) and response of the adjacent Pacific Ocean. Scientific
681 Reports 6, 21064.
- 682 Haberle, S.G., Bennett, K.D., 2004. Postglacial formation and dynamics of North Patagonian
683 Rainforest in the Chonos Archipelago, Southern Chile. Quaternary Science Reviews 23, 2433-
684 2452.
- 685 Hall, B.L., Porter, C.T., Denton, G.H., Lowell, T.V., Bromley, G.R.M., 2013. Extensive recession of
686 Cordillera Darwin glaciers in southernmost South America during Heinrich Stadial 1.
687 Quaternary Science Reviews 62, 49-55.



- 688 Hein, A.S., Hulton, N.R.J., Dunai, T.J., Sugden, D.E., Kaplan, M.R., Xu, S., 2010. The chronology of
689 the Last Glacial Maximum and deglacial events in central Argentine Patagonia. *Quaternary*
690 *Science Reviews* 29, 1212-1227.
- 691 Heiri, O., Lotter, A.F., Lemcke, G., 2001. Loss on ignition as a method for estimating organic and
692 carbonate content in sediments: reproducibility and comparability of results. *Journal of*
693 *Paleolimnology* 25, 101-110.
- 694 Heusser, C.J., 1971. *Pollen and Spores from Chile*. University of Arizona Press, Tucson.
- 695 Higuera, P.E., Brubaker, L.B., Anderson, P.M., Hu, F.S., Brown, T.A., 2009. Vegetation mediated the
696 impacts of postglacial climate change on fire regimes in the south-central Brooks Range,
697 Alaska. *Ecological Monographs* 79, 201-219.
- 698 Kaplan, M.R., Strelin, J.A., Schaefer, J.M., Denton, G.H., Finkel, R.C., Schwartz, R., Putnam, A.E.,
699 Vandergoes, M.J., Goehring, B.M., Travis, S.G., 2011. In-situ cosmogenic ^{10}Be production
700 rate at Lago Argentino, Patagonia: Implications for late-glacial climate chronology. *Earth and*
701 *Planetary Science Letters* 309, 21-32.
- 702 Kaufman, D.S., Ager, T.A., Anderson, N.J., Anderson, P.M., Andrews, J.T., Bartlein, P.J., Brubaker,
703 L.B., Coats, L.L., Cwynar, L.C., Duvall, M.L., Dyke, A.S., Edwards, M.E., Eisner, W.R., Gajewski,
704 K., Geirsdottir, A., Hu, F.S., Jennings, A.E., Kaplan, M.R., Kerwin, M.N., Lozhkin, A.V.,
705 MacDonald, G.M., Miller, G.H., Mock, C.J., Oswald, W.W., Otto-Bliesner, B.L., Porinchu, D.F.,
706 Ruhland, K., Smol, J.P., Steig, E.J., Wolfe, B.B., 2004. Holocene thermal maximum in the
707 western Arctic (0-180 degrees W). *Quaternary Science Reviews* 23, 529-560.
- 708 Luebert, F., Plischoff, P., 2006. *Sinopsis Bioclimática y Vegetacional de Chile*. Editorial Universitaria,
709 Santiago, Chile.
- 710 Lumley, S., Switsur, R., 1993. Late Quaternary chronology of the Taitao Peninsula, Southern Chile. .
711 *Journal of Quaternary Science* 8, 161-165.
- 712 Mancini, M.V., 2002. Vegetation and climate during the holocene in Southwest Patagonia,
713 Argentina. *Review of Palaeobotany and Palynology* 122, 101-115.
- 714 Markgraf, V., Whitlock, C., Haberle, S., 2007. Vegetation and fire history during the last 18,000 cal
715 yr BP in Southern Patagonia: Mallin Pollux, Coyhaique, Province Aisen (45 degrees 41 ' 30 " S,
716 71 degrees 50 ' 30 " W, 640 m elevation). *Palaeogeography Palaeoclimatology*
717 *Palaeoecology* 254, 492-507.
- 718 Moreno, P.I., Denton, G.H., Moreno, H., Lowell, T.V., Putnam, A.E., Kaplan, M.R., 2015.
719 Radiocarbon chronology of the last glacial maximum and its termination in northwestern
720 Patagonia. *Quaternary Science Reviews* 122, 233-249.
- 721 Moreno, P.I., Francois, J.P., Villa-Martínez, R., Moy, C.M., 2010. Covariability of the Southern
722 Westerlies and atmospheric CO_2 during the Holocene. *Geology* 39, 727-730.
- 723 Moreno, P.I., Kaplan, M.R., Francois, J.P., Villa-Martínez, R., Moy, C.M., Stern, C.R., Kubik, P.W.,
724 2009. Renewed glacial activity during the Antarctic cold reversal and persistence of cold
725 conditions until 11.5 ka in southwestern Patagonia. *Geology* 37, 375-378.
- 726 Moreno, P.I., Vilanova, I., Villa-Martínez, R., Garreaud, R.D., Rojas, M., De Pol-Holz, R., 2014.
727 Southern Annular Mode-like changes in southwestern Patagonia at centennial timescales
728 over the last three millennia. *Nat Commun* 5.
- 729 Moreno, P.I., Villa-Martínez, R., Cardenas, M.L., Sagredo, E.A., 2012. Deglacial changes of the
730 southern margin of the southern westerly winds revealed by terrestrial records from SW
731 Patagonia (52 degrees S). *Quaternary Science Reviews* 41, 1-21.
- 732 Pesce, O.H., Moreno, P.I., 2014. Vegetation, fire and climate change in central-east Isla Grande de
733 Chiloé (43°S) since the Last Glacial Maximum, northwestern Patagonia. *Quaternary Science*
734 *Reviews* 90, 143-157.



- 735 Pisano, E., 1997. Los bosques de Patagonia Austral y Tierra del Fuego chilenas. *Anales del Instituto*
736 *de la Patagonia, Serie Ciencias Naturales (Chile)* 25, 9:19.
- 737 Schmithüsen, J., 1956. Die raumliche Ordnung der chilenischen Vegetation. *Bonner Geographische*
738 *Abhandlungen* 17, 1-86.
- 739 Stenni, B., Masson-Delmotte, V., Selmo, E., Oerter, H., Meyer, H., Rothlisberger, R., Jouzel, J.,
740 Cattani, O., Falourd, S., Fischer, H., Hoffmann, G., Iacumin, P., Johnsen, S.J., Minster, B.,
741 Udisti, R., 2010. The deuterium excess records of EPICA Dome C and Dronning Maud Land
742 ice cores (East Antarctica). *Quaternary Science Reviews* 29, 146-159.
- 743 Stern, C., 2004. Active Andean volcanism: its geologic and tectonic setting. *Revista Geológica de*
744 *Chile* 31, 161-206.
- 745 Stern, C.R., Moreno, P.I., Henriquez, W.I., Villa-Martinez, R., Sagredo, E., Aravena, J.C., De Pol-Holz,
746 R., 2016. Holocene tephrochronology around Cochrane (~47°S), southern Chile. *Andean*
747 *Geology* 43, 1-19.
- 748 Strelin, J.A., Denton, G.H., Vandergoes, M.J., Ninnemann, U.S., Putnam, A.E., 2011. Radiocarbon
749 chronology of the late-glacial Puerto Bandera moraines, Southern Patagonian Icefield,
750 Argentina. *Quaternary Science Reviews* 30, 2551-2569.
- 751 Strelin, J.A., Malagnino, E.C., 2000. Late-Glacial History of Lago Argentino, Argentina, and Age of
752 the Puerto Bandera Moraines. *Quaternary Research* 54, 339-347.
- 753 Turner, K.J., Fogwill, C.J., McCulloch, R.D., Sugden, D.E., 2005. Deglaciation of the eastern flank of
754 the North Patagonian Icefield and associated continental-scale lake diversions. *Geografiska*
755 *Annaler: Series A, Physical Geography* 87, 363-374.
- 756 Villa-Martinez, R., Moreno, P.I., Valenzuela, M.A., 2012. Deglacial and postglacial vegetation
757 changes on the eastern slopes of the central Patagonian Andes (47 degrees S). *Quaternary*
758 *Science Reviews* 32, 86-99.

759

760



761 Table 1

Laboratory code	Core	Material	Length (cm)	14C yr BP \pm 1 σ	Median probability (cal yr BP)	2 σ range (cal BP)
UCIAMS-133501	PC0902AT7	Bulk	660-661	8935 \pm 25	10,029	9794-10,177
UCIAMS-133416	PC0902AT8	Bulk	705-706	11,350 \pm 60	13,229	13,109-13,350
UCIAMS-133417	PC0902AT8	Bulk	757-758	13,740 \pm 70	16,863	16,684-17,055
UCIAMS-133418	PC0902AT8	Bulk	795-796	16,250 \pm 90	19,414	18,934-19,779
CAMS-144454	PC0902BT8	Bulk	795-796	16,020 \pm 50	19,164	18,922-19,408

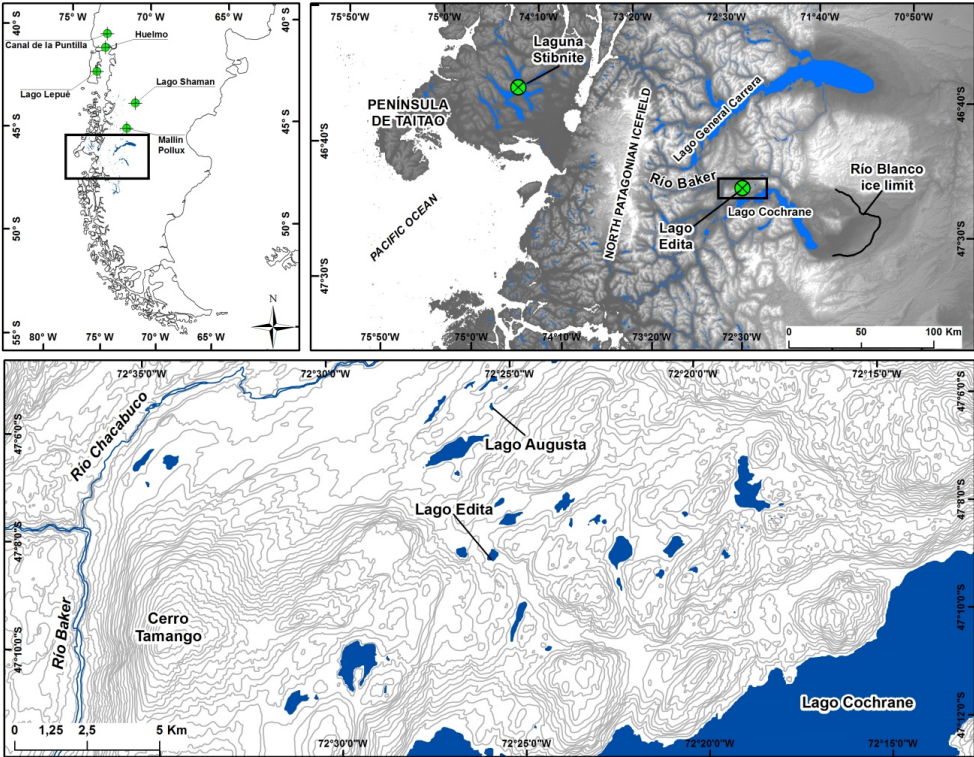
762

763



764 Figure 1

765



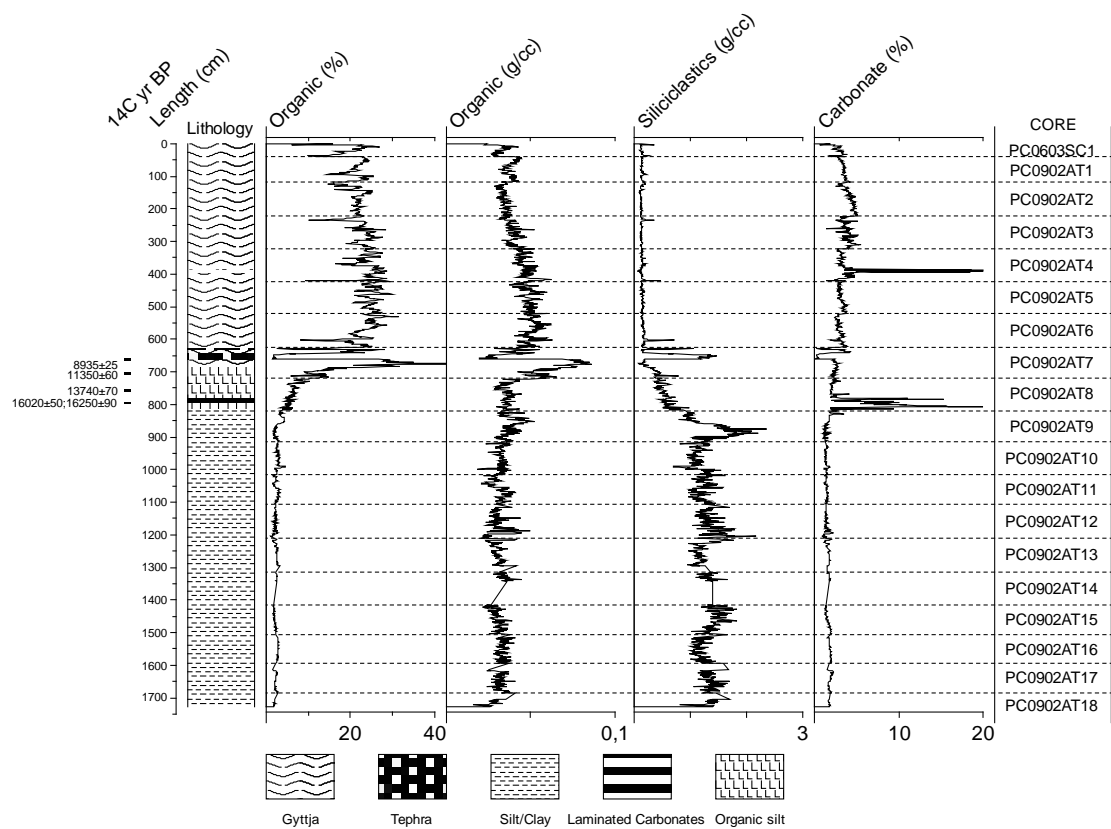
766

767





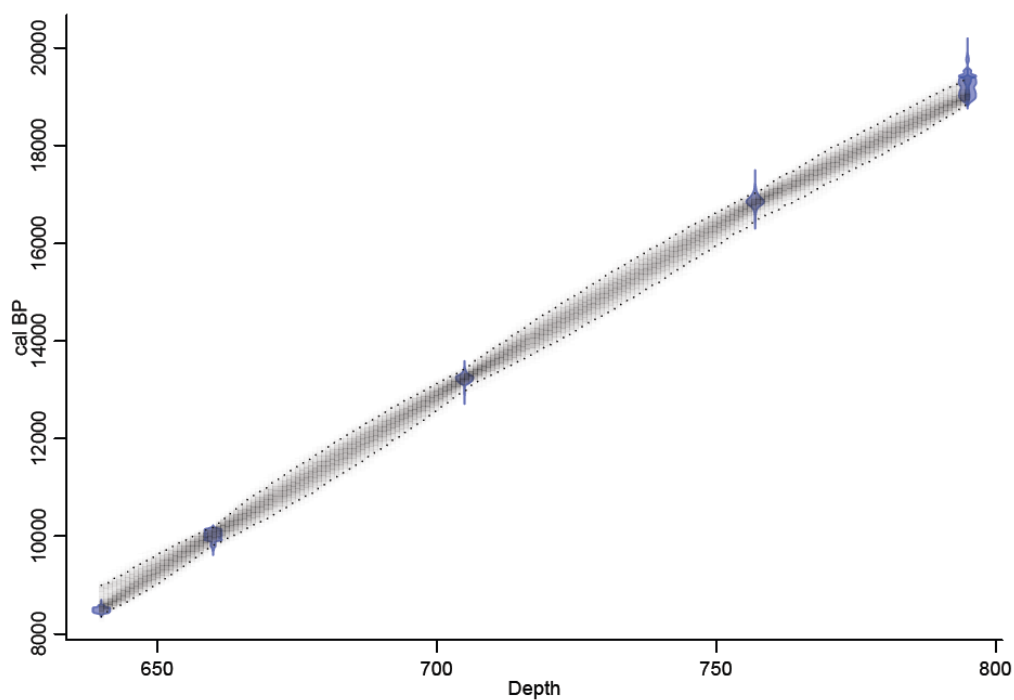
Figure 2





777 Figure 3

778



779

780

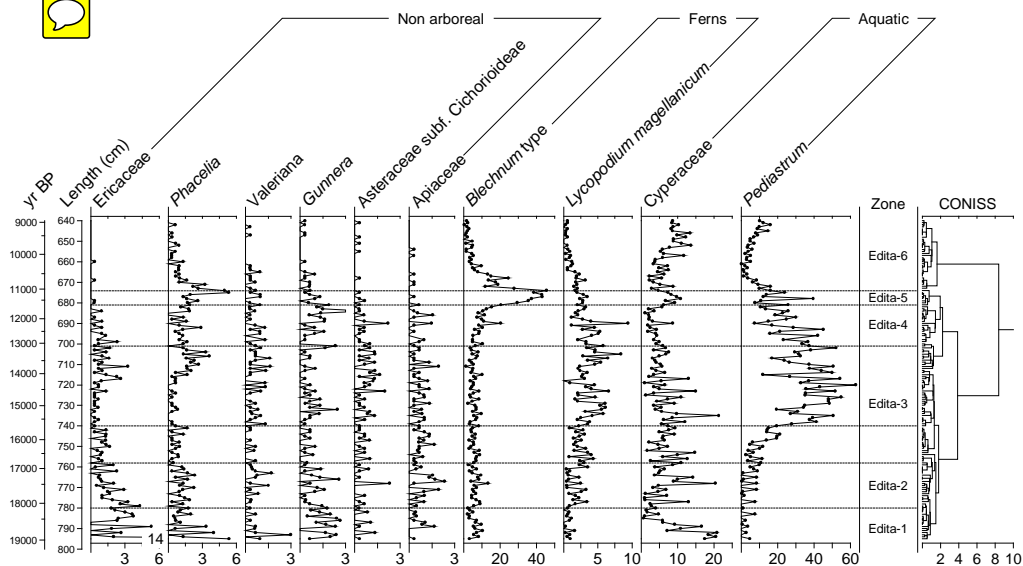
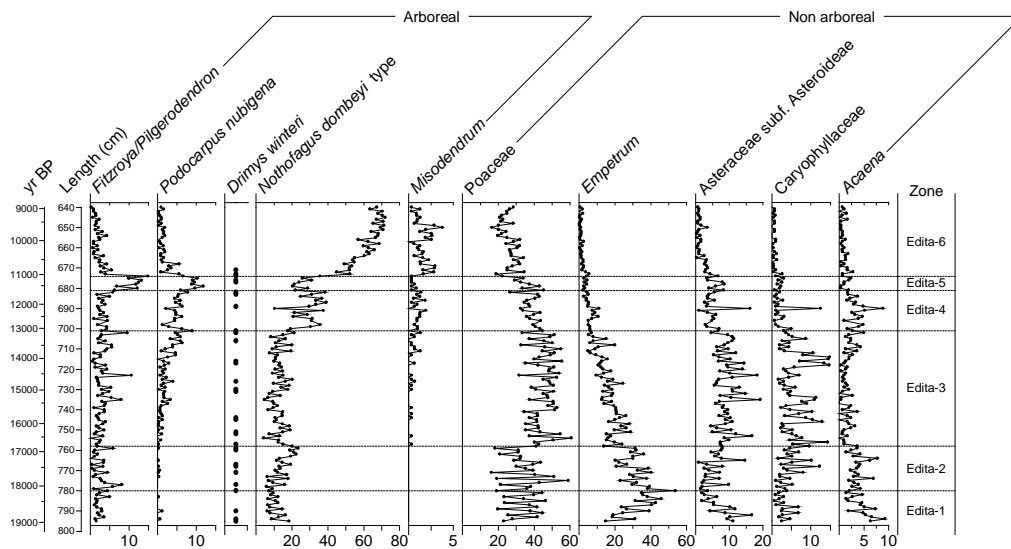




781 Figure 4

782

783



784



785 Figure 5

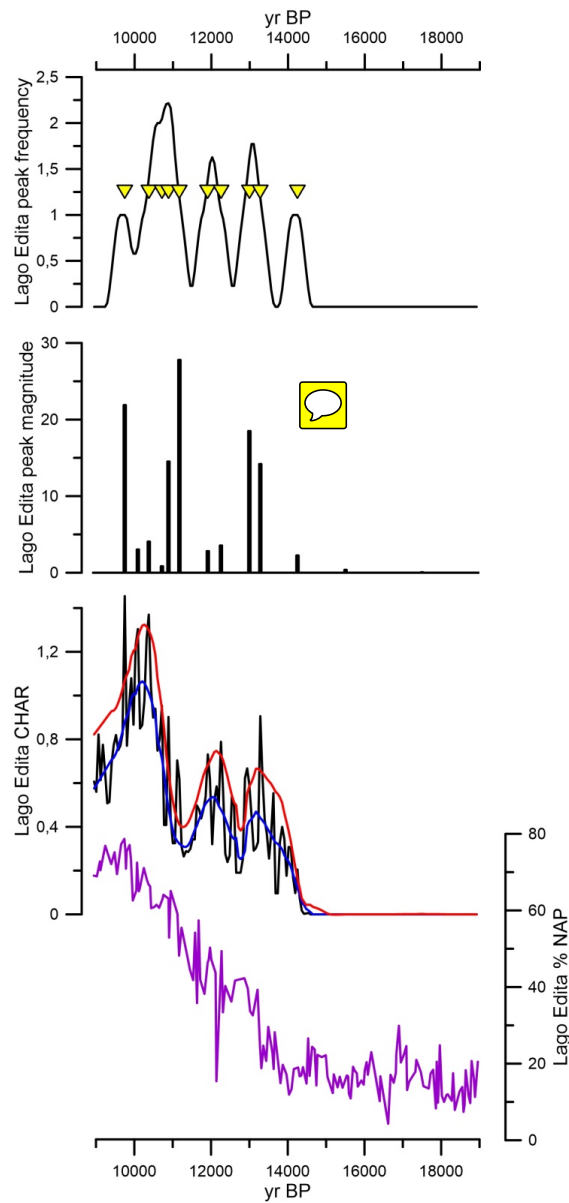
786

787

788

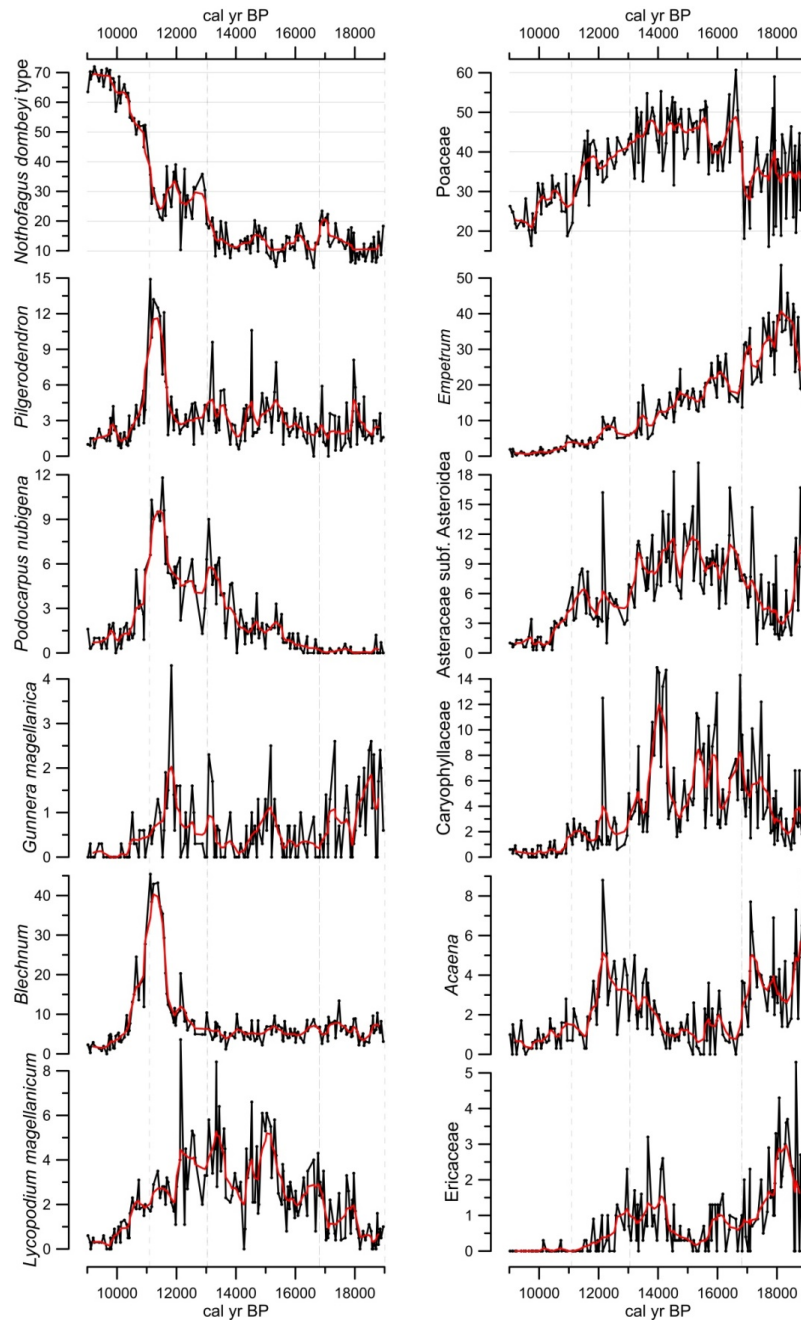
789

790





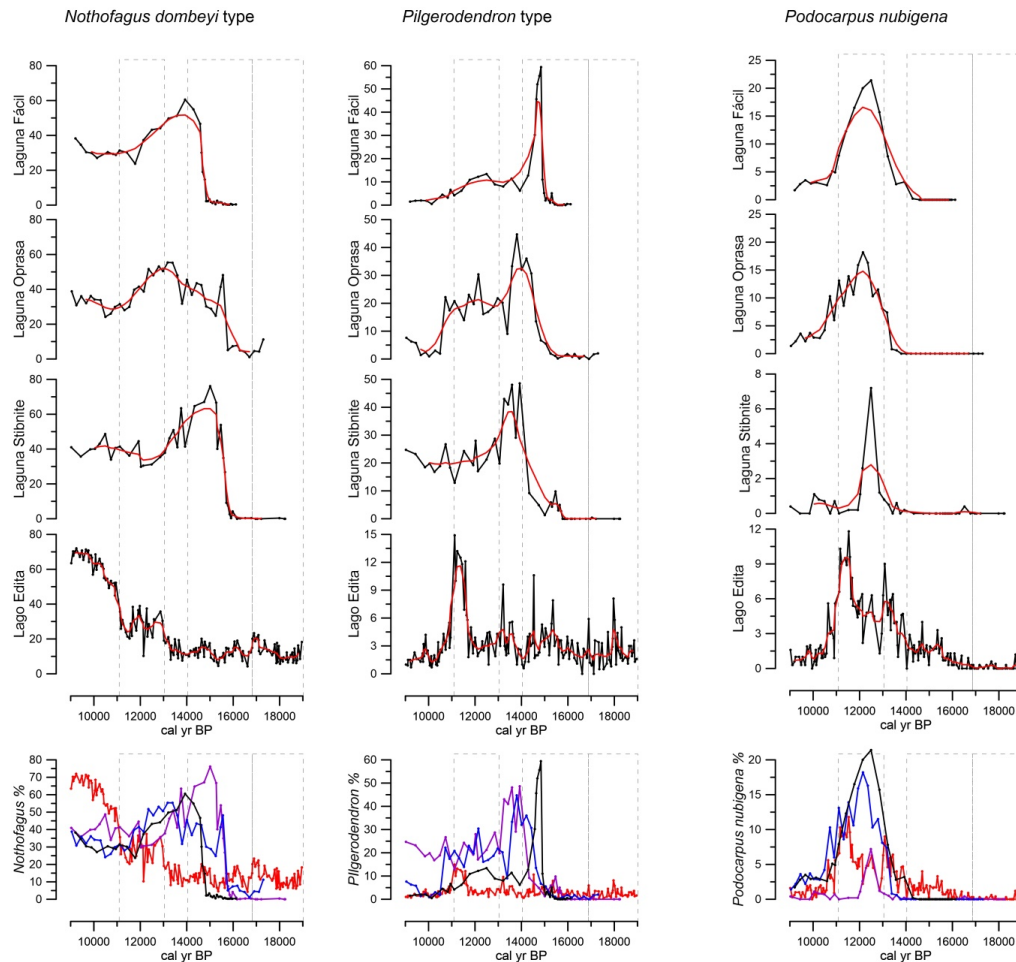
791 Figure 6



792



793 Figure 7



794

795

796



797 Figure 8

798

799

